To cite this version :

Influence of Poroelasticity of the Surface Layer on the Surface Love Wave Propagation

Adil El Baroudi
LAMPA Engineering Laboratory Arts &
Métiers ParisTech,
Angers 49035, France
e-mail: adil.elbaroudi@ensam.eu

This work presents a theoretical method for surface love waves in poroelastic media loaded with a viscous fluid. A complex analytic form of the dispersion equation of surface love waves has been developed using an original resolution based on pressure–displacement formulation. The obtained complex dispersion equation was separated in real and imaginary parts. MATHEMATICA *software was used to solve the resulting nonlinear system of equations. The effects of surface layer porosity and fluid viscosity on the phase velocity and the wave attenuation dispersion curves are inspected. The numerical solu-tions show that the wave attenuation and phase velocity variation strongly depend on the fluid viscosity, surface layer porosity, and wave frequency. To validate the original theo-retical resolution, the results in literature in the case of an homogeneous isotropic sur-face layer are used. The results of various investigations on love wave propagation can serve as benchmark solutions in design of fluid viscosity sensors, in nondestructive testing (NDT) and geophysics.* [DOI: 10.1115/1.4039336]

1 Introduction

Surface love waves in a layered medium have been successfully applied in many fields like nondestructive testing (NDT) and material characterization [1–3], seismology, and earthquake engineering [4–9]. Recently, the use of love waves devices for the development of viscosity sensors [10–15], chemical sensors [16], and biosensors [17–20] has been extensively investigated.

Surface love waves propagate in a layered structure consisting of an elastic substrate and a surface layer. The necessary condition for that the love waves in an homogeneous structure exist, the velocity of the bulk shear wave propagation in the surface layer have to be less than that in the substrate. In addition, surface love wave that have only one mechanical displacement component is a transverse surface wave. This displacement is parallel to the surface and perpendicular to the direction of propagation.

Acoustic surface waves propagation in elastic structure (waveguide) loaded by a viscous fluid have attracted attention of a number of scientists [21–26]. Nevertheless, a detailed quantitative analytical approach of surface love wave in poroelastic structure covered with a viscous fluid is still lacking.

In this paper, since the waveguide surface is loaded by a viscous fluid, surface love waves undergo significant attenuation mainly due to the viscosity; hence, the wave number takes a complex form. The real part of this wave number defines the love wave phase velocity, while the imaginary part represents the love wave attenuation coefficient.

A new rigorous, efficient, and reliable mathematical method based on a pressure–displacement formulation, to be able to accurately predict the behavior of love wave, taking into account the poroelastic character of the surface layer remains a daunting task and is the purpose of the present paper. The effect of fluid dynamic viscosity and surface porosity on the attenuation and phase velocity of surface love waves are investigated. The obtained results of various investigations on love wave propagation in this work can provide interesting information, for example, to develop love-wave-based devices. Note that this paper is based on the results and methodology presented in work [26].

2 Formulation and Mathematical Analysis

2.1 Physical Model Description. The waveguide structure that guides love waves consists of a poroelastic surface layer deposited on a perfect elastic substrate as shown in Fig. 1. The surface of the waveguide layer ($x_2 = -d$) is loaded with a viscous fluid ($x_2 < -d$). The displacement component u_3 of the surface love wave propagating in the waveguide structure is polarized along the x_3-axis and perpendicular to the propagation direction x_1. The two-dimensional problem in Cartesian coordinates with no variation along the x_3-axis of the geometry is considered. Although surface love waves exhibit a multimode character, the fundamental mode plays an important role in many applications such as NDT and sensors. Accordingly, in this paper, the attention is focused on the properties of the fundamental love waves' mode. Note that when the porosity tends to zero, the physical model described in this paper were identical to the one presented by Kielczynski et al. [26]. In addition, the propagation loss is due only to the fluid viscosity.
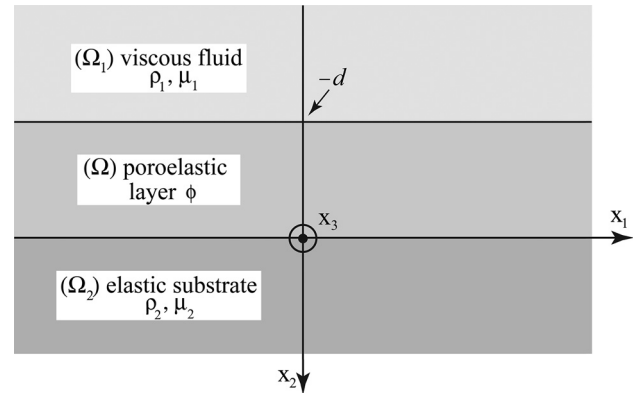

Fig. 1 Schematic representation of the surface love wave waveguide. *d* and ϕ are, respectively, the thickness and porosity of the surface layer (domain Ω). μ_1 and ρ_1 are, respectively, the dynamic viscosity and density of the fluid (domain Ω_1). μ_2 and ρ_2 correspond to the shear modulus and density of the elastic substrate (domain Ω_2), respectively. Surface love waves that propagate in the *x_1*-direction are polarized along the *x_3*-axis.

2.2 Viscous Fluid Domain. The fluid under consideration will behave as a nonconductive viscous fluid. The fluid motion is only produced by wave propagation in the poroelastic media. Here, the nonlinear convective term can be neglected in the Navier–Stokes equations. Furthermore, since only shear deformation arises during transverse waves propagation, we can also ignore the pressure gradient [27]. Thus, the linearized Navier–Stokes equation governs the viscous fluid motion can be simplified to the following:

$$\frac{1}{\nu_1}\frac{\partial v_3}{\partial t} = \frac{\partial^2 v_3}{\partial x_1^2} + \frac{\partial^2 v_3}{\partial x_2^2} \qquad (1)$$

where $\nu_1 = \mu_1/\rho_1$ is the kinematic fluid viscosity and v_3 is the velocity field in a viscous fluid in the x_3-direction.

2.3 Poroelastic Surface Layer. A poroelastic surface layer is composed of a pore spaces and solid skeleton. The pore spaces enable the filtration of fluid through poroelastic surface layer. The solid skeleton consists of the solid matrix with pores in between. The stress–strain constitutive relation based on Biot's poroelastic theory [28–31] is

$$\boldsymbol{\sigma} = \lambda e \mathbf{I} + \mu[\nabla \mathbf{u} + (\nabla \mathbf{u})^{\mathrm{T}}] - \alpha p \mathbf{I} \qquad (2)$$

where $\boldsymbol{\sigma}$ represents the stress tensor, λ is the Lamé parameter, $e = \nabla \cdot \mathbf{u}$ is the solid skeleton dilatation, $\mathbf{u}$ is the displacement field in the solid skeleton, $\mathbf{I}$ is the identity tensor, μ is the shear modulus of the porous framework, p is the pore fluid pressure, and α is the Biot-Willis coefficient [32]. A second constitutive relation for the pore fluid pressure is given by

$$p = -\alpha M e + M\zeta \qquad (3)$$

where $\zeta = -\nabla \cdot \mathbf{w}$ is the volume variations in the fluid [30], $\mathbf{w} = \phi(\mathbf{u}^f - \mathbf{u})$ is the relative displacement of the fluid with respect to the solid skeleton, and $\mathbf{u}^f$ and ϕ denote, respectively, the pore fluid displacement field and the surface porosity. In Eq. (3), M is the Biot scalar modulus [32]. Furthermore, M and α can be expressed in terms of three elastic modulus [33,34]: the matrix bulk modulus K_m, the solid bulk modulus K_s, and the pore fluid bulk modulus K_f. The resulting equations for M and α are

$$\frac{1}{M} = \frac{\phi}{K_f} + \frac{\alpha - \phi}{K_s}, \quad \alpha = 1 - \frac{K_m}{K_s} \qquad (4)$$

Note that M is defined physically as the ratio of ζ to pore fluid pressure measured under the condition of constant solid skeleton dilatation and the Biot-Willis coefficient α is equal to the ratio of ζ to e measured with p held constant [32].

The Biot [28–31] coupled equation can be expressed in the form

$$\rho\frac{\partial^2 \mathbf{u}}{\partial t^2} + \rho_f\frac{\partial^2 \mathbf{w}}{\partial t^2} = \nabla \cdot \boldsymbol{\sigma} \qquad (5)$$

where ρ_f is the pore fluid density and $\rho = \phi\rho_f + (1 - \phi)\rho_s$ represents the mixture density. The coupled motion of the pore fluid with respect to the solid skeleton in the absence of body forces is governed by the generalized Darcy's law [28]

$$\rho_f\frac{\partial^2 \mathbf{u}}{\partial t^2} + \frac{\rho_f \tau}{\phi}\frac{\partial^2 \mathbf{w}}{\partial t^2} + \frac{\eta}{k}\frac{\partial \mathbf{w}}{\partial t} = -\nabla p \qquad (6)$$

where η is the dynamic viscosity of pore fluid and k is the permeability of porous media. The tortuosity parameter τ describes how much the orientation of the pores restricts fluid flow to lead to an inertial coupling [35]. Note that, in the case where the pores are uniform and parallel to the direction of fluid flow, $\tau = 1$ and no inertial coupling occurs. In the Eq. (6), the viscous and inertial coupling between the solid and fluid phases are represented by the parameters $(\eta/k) = b$ and $(\rho_f\tau/\phi) = m$, respectively [28,30].

2.3.1 Pressure–Displacement $p - \mathbf{u}$ Formulation. This work focuses solely on solving analytically the Biot equations in the $p - \mathbf{u}$ formulation. Indeed, applying the operator $\nabla\cdot$ (Divergence) to both sides of Eq. (6) and taking into account Eq. (3), we get the first following coupled Biot equation expressed in terms of the field variables p and $\mathbf{u}$

$$\nabla^2 p - \frac{m}{M}\frac{\partial^2 p}{\partial t^2} - \frac{b}{M}\frac{\partial p}{\partial t} + \left[(\rho_f - \alpha m)\frac{\partial^2}{\partial t^2} - \alpha b\frac{\partial}{\partial t}\right]\nabla \cdot \mathbf{u} = 0 \qquad (7)$$

In order to obtain the second coupled Biot equation expressed in terms of the field variables p and $\mathbf{u}$, first we apply the $\partial/\partial t$ operator to both sides of Eq. (6); its result and Eq. (5) can be combined taking into account the constitutive relation (2) to give

$$\left(b + m\frac{\partial}{\partial t}\right)\left[\mu\nabla^2\mathbf{u} + (\lambda + \mu)\nabla\nabla \cdot \mathbf{u}\right]$$
$$-\left[b\rho + \left(m\rho - \rho_f^2\right)\frac{\partial}{\partial t}\right]\frac{\partial^2\mathbf{u}}{\partial t^2} \qquad (8)$$
$$-\left[b\alpha + (m\alpha - \rho_f)\frac{\partial}{\partial t}\right]\nabla p = 0$$

To plainly introduce the displacement field in terms of potentials for the $p - \mathbf{u}$ formulation, the vector $\mathbf{u}$ can advantageously be decomposed using Helmholtz decomposition. In this work, the propagation of plane harmonic waves in x_1-direction is considered; thus, all physical quantities such as displacement field and stress vector are independent of x_3 and depend only on in-plane variables (x_1, x_2). Therefore, the displacement field can be shown to be [36]

$$u_3 = -\frac{\partial^2 \psi}{\partial x_1^2} - \frac{\partial^2 \psi}{\partial x_2^2} \qquad (9)$$

Introducing Eq. (9) into Eqs. (7) and (8) after some elementary manipulation yields

$$\mu\left(b + m\frac{\partial}{\partial t}\right)\left(\frac{\partial^2\psi}{\partial x_1^2} + \frac{\partial^2\psi}{\partial x_2^2}\right) - \left[b\rho + \left(m\rho - \rho_f^2\right)\frac{\partial}{\partial t}\right]\frac{\partial^2\psi}{\partial t^2} = 0 \qquad (10)$$

2.4 Elastic Substrate. Based on the elastodynamic theory, the equation of motion of the surface guided wave in homogeneous, isotropic elastic substrate can be established. The displacement field of the elastic substrate is governed by the Navier's equation [37]

$$\frac{1}{c_2^2}\frac{\partial^2 u_3^{(2)}}{\partial t^2} = \frac{\partial^2 u_3^{(2)}}{\partial x_1^2} + \frac{\partial^2 u_3^{(2)}}{\partial x_2^2} \qquad (11)$$

where $c_2 = \sqrt{\mu_2/\rho_2}$ is the shear wave velocity in the elastic substrate and $u_3^{(2)}$ the elastic substrate particle displacement in the x_3-direction.

2.5 General Solution of Wave Propagation. For a propagation of plane harmonic waves in x_1-direction, the solution of Eqs. (1), (10), and (11) of the velocity field v_3 in the viscous fluid, scalar potential ψ in the poroelastic surface, and of the displacement field $u_3^{(2)}$ in the elastic substrate are sought in the form

$$\begin{Bmatrix} v_3 \\ \psi \\ u_3^{(2)} \end{Bmatrix}(x_2, x_1, t) = \begin{Bmatrix} V(x_2) \\ \Psi(x_2) \\ U(x_2) \end{Bmatrix} \exp\left\{ j[(k_r + jk_i)x_1 - \omega t] \right\} \quad (12)$$

where ω is the angular frequency and $j = \sqrt{-1}$, k_r is the real part of the wave number that determines the love wave phase velocity, and k_i is the imaginary part of the wave number that represents the love wave attenuation coefficient. Substituting Eq. (12) into Eqs. (1), (10), and (11) and using previously developed techniques [37], the x_2 dependence can be expressed as

$$V(x_2) = C_1 \exp(\delta_1 x_2)$$
$$\Psi(x_2) = C_2 \sin(\delta x_2) + C_3 \cos(\delta x_2) \quad (13)$$
$$U(x_2) = C_4 \exp(-\delta_2 x_2)$$

where

$$\delta_1^2 = k_r^2 - k_i^2 - j\left(\frac{\omega}{\nu_1} - 2k_r k_i\right) \quad (14)$$

$$\delta^2 = \omega^2\left(\frac{\rho}{\mu} - \frac{m\rho_f^2}{\mu\left(m^2 + \dfrac{b^2}{\omega^2}\right)}\right) - k_r^2 + k_i^2$$

$$+ j\left(\frac{\omega b\rho_f^2}{\mu\left(m^2 + \dfrac{b^2}{\omega^2}\right)} - k_r k_i\right) \quad (15)$$

$$\delta_2^2 = k_r^2 - k_i^2 - \frac{\omega^2}{c_2^2} + 2jk_r k_i \quad (16)$$

and C_1, C_2, C_3, and C_4 are arbitrary constants. To assure that the love wave amplitude in viscous fluid decays to zero with increasing distance from the waveguide surface $x_2 \to -\infty$, $\mathrm{Re}(\delta_1)$ must be greater than zero. To assure that the love wave amplitude in substrate decays to zero, when $x_2 \to \infty$, $\mathrm{Re}(\delta_2)$ must be greater than zero. In addition, the shear stress components are given by

$$\begin{Bmatrix} \sigma_{23}^{(1)} \\ \sigma_{23} \\ \sigma_{23}^{(2)} \end{Bmatrix} = \begin{Bmatrix} \mu_1 \partial_{x_2} v_3 \\ \mu \partial_{x_2} u_3 \\ \mu_2 \partial_{x_2} u_3^{(2)} \end{Bmatrix} = \begin{Bmatrix} \mu_1 \Sigma_1(x_2) \\ \mu \Sigma(x_2) \\ \mu_2 \Sigma_2(x_2) \end{Bmatrix} \exp\left\{ j[(k_r + jk_i)x_1 - \omega t] \right\}$$

$$(17)$$

where the x_2 dependence is defined as

$$\Sigma_1(x_2) = C_1 \delta_1 \exp(\delta_1 x_2)$$
$$\Sigma(x_2) = \delta\left[\delta^2 + (k_r + jk_i)^2\right][C_2 \cos(\delta x_2) - C_3 \sin(\delta x_2)]$$
$$\Sigma_2(x_2) = -C_4 \delta_2 \exp(-\delta_2 x_2)$$

2.6 Boundary and Interface Conditions. To determine the arbitrary constants C_1, C_2, C_3, and C_4 in the earlier expressions, we apply the following boundary conditions on the $x_2 = -d$ and $x_2 = 0$. They are continuity of shear stress and continuity of mechanical displacement

(1) At the interface between the viscous fluid and the poroelastic layer ($x_2 = -d$), the velocity and stress should be continuous

$$\left(v_3 - \frac{\partial u_3}{\partial t}\right)_{x_2 = -d} = 0$$

$$\left(\sigma_{23}^{(1)} - \sigma_{23}\right)_{x_2 = -d} = 0 \quad (18)$$

(2) At the interface between the elastic substrate and the poroelastic layer ($x_2 = 0$), the displacement and stress should be continuous

$$\left(u_3 - u_3^{(2)}\right)_{x_2 = 0} = 0$$

$$\left(\sigma_{23} - \sigma_{23}^{(2)}\right)_{x_2 = 0} = 0 \quad (19)$$

Equations (18) and (19) result in a system of four linear algebraic equations in four unknown coefficients C_i. Furthermore, for a nontrivial solution, the determinant of this system must be equal to zero to lead to the following complex dispersion relation (CDR)

$$\mathrm{CDR} = \left(\mu^2 \delta^2 + j\omega\mu_1\mu_2\delta_1\delta_2\right)\sin(\delta d)$$
$$+ \mu\delta(j\omega\mu_1\delta_1 - \mu_2\delta_2)\cos(\delta d) = 0 \quad (20)$$

where δ, δ_1, and δ_2 are complex. Eq. (20) represents the CDR of surface love waves propagating in poroelastic layer loaded with a viscous fluid. Separating the imaginary and real parts of CDR, we obtain a system of nonlinear equations given in Appendix with unknowns k_r and k_i. This system was solved using MATHEMATICA software. After finding the roots (k_r, k_i), the love wave phase velocity $v_p = \omega/k_r$ can be calculated. While the root k_i represents the love wave attenuation in the direction of propagation.

2.7 Numerical Example. The material properties were used in the numerical computations were derived from Ref. [26] for the elastic substrate and from Ref. [38] for the poroelastic surface. The poroelastic surface layer thickness d was 0.4 (mm). In this work, the viscosity of the fluid is the only source of losses. Numerical calculation is performed in the dynamic viscosity range from 0.01 to 100 (Pa·s), for values of frequency from 0.5 to 5 (MHz) and for three values of porosity 0, 0.1, and 0.5. Thus, the material parameters used in the numerical computation are given in Table 1.

The numerical results of attenuation and wave phase velocity are shown in Figs. 2–14. To validate the new original theoretical resolution, the results of Ref. [26] in the case of an elastic surface layer which corresponds to $\phi \to 0$ in this study are used. The following concluding remarks can be drawn:

- Figures 2–7 show the influence of the fluid dynamic viscosity on the love wave phase velocity for two frequencies ($f = 1$ and 5 (MHz)) and for three values of porosity ($\phi \to 0, 0.1$, and 0.5). It can be seen from Figs. 2, 4, and 6 that the phase velocity decreases with increasing in dynamic viscosity.

Table 1 Material parameters

Properties	Substrate
μ_2	8.02×10^{10} (Pa)
ρ_2	7800 (kg/m³)
Properties	**Poroelastic layer**
K_s	35×10^9 (Pa)
K_f	2.2×10^9 (Pa)
K_m	5×10^9 (Pa)
μ	3.91×10^{10} (Pa)
ρ_s	8900 (kg/m³)
ρ_f	1000 (kg/m³)
k	2.4×10^{-11} (m²)
τ	3
ϕ	$0.001, 0.1, 0.5$
Properties	**Viscous liquid**
ρ_1	1000 (kg/m³)
μ_1	$\in [0.01, 100]$ (Pa·s)

Fig. 2 Phase velocity dispersion curve versus dynamic viscosity of fluid for $f = 1$ (MHZ) in the case of an elastic surface layer

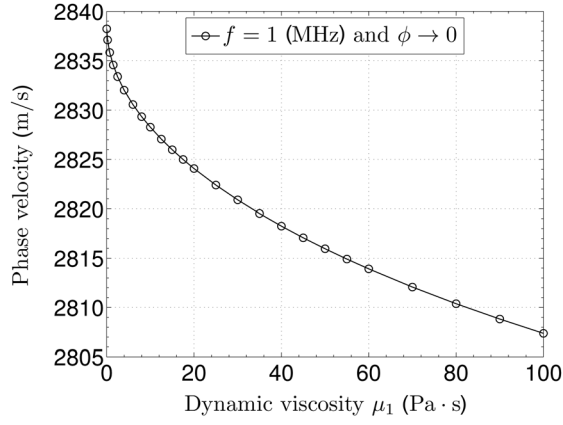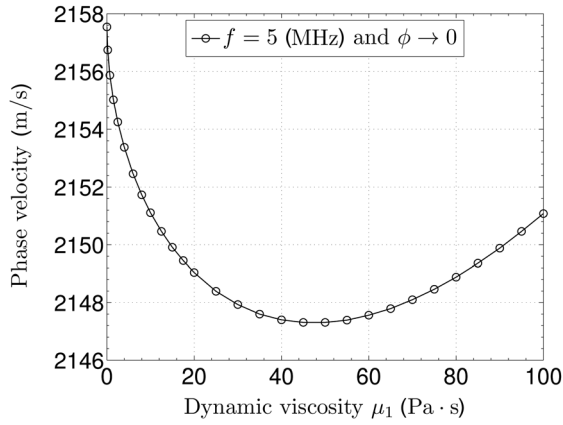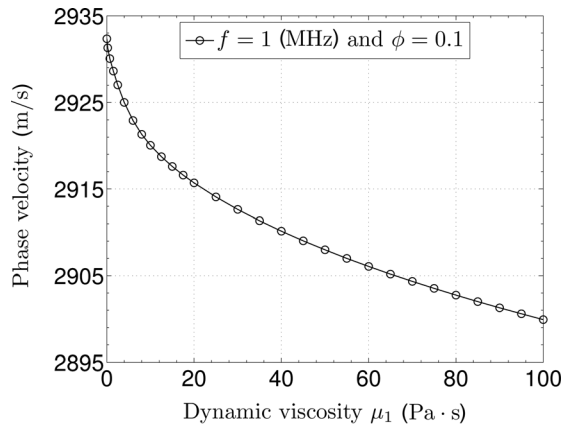**Fig. 5** Phase velocity dispersion curve versus dynamic viscosity of fluid for $f = 5$ (MHZ) in the case of a poroelastic surface layer
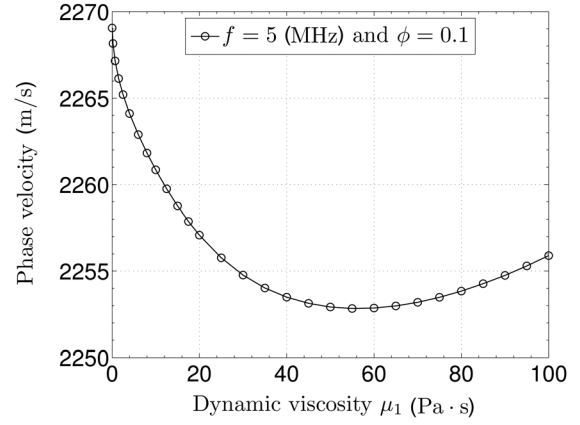
However, for higher frequency $\left(f = 5\,(\mathrm{MHz})\right)$, with an increase in dynamic viscosity, the love wave phase velocity first decreases and then augments (3, 5, and 7). Guo and Sun [25] have observed a similar phenomenon in the case of Bleustein–Gulyaev waves propagation. These waves propagate in the metallized piezoelectric layer and are a surface acoustic waves. To explain this phenomenon, the very viscous fluid that loads the waveguide surface may be tends to increase the material stiffness of the surface layer causing an increase in the love wave phase velocity.

- Figures 9–11 illustrate the influence of the fluid dynamic viscosity on the dispersion curves of phase velocity for viscosities $\mu_1 = 0.01$, 10, and 50 (Pa·s). Figures 9–11 indicate that with an increase in dynamic viscosity, the phase velocity decreases. Note that in the case of an elastic surface layer $(\phi \to 0)$, Fig. 9 is identical to that of Ref. [26].

Fig. 3 Phase velocity dispersion curve versus dynamic viscosity of fluid for $f = 5$ (MHZ) in the case of an elastic surface layer

Fig. 6 Phase velocity dispersion curve versus dynamic viscosity of fluid for $f = 1$ (MHZ) in the case of a poroelastic surface layer
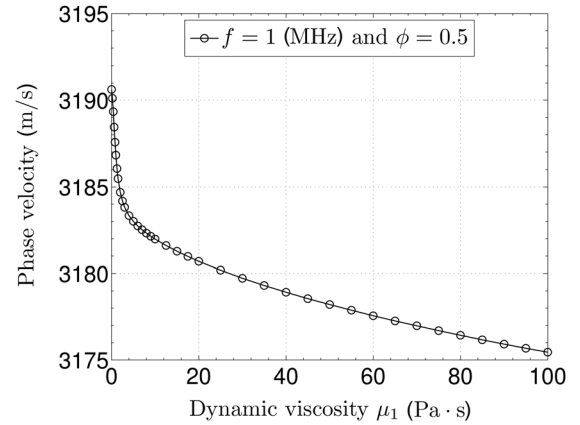

Fig. 4 Phase velocity dispersion curve versus dynamic viscosity of fluid for $f = 1$ (MHZ) in the case of a poroelastic surface layer

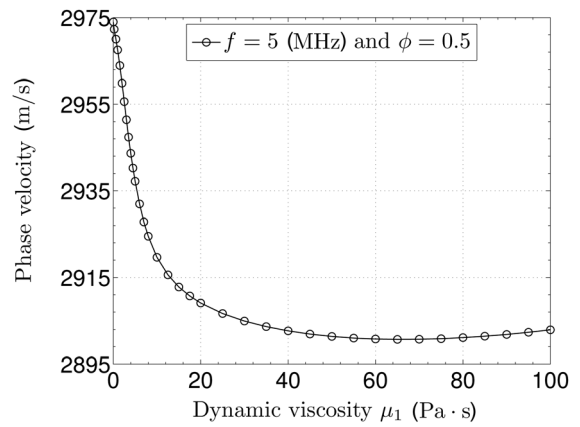**Fig. 7** Phase velocity dispersion curve versus dynamic viscosity of fluid for $f = 5$ (MHZ) in the case of a poroelastic surface layer
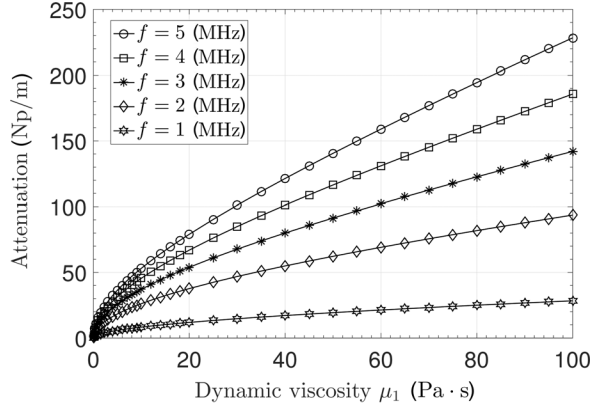
Fig. 8 Attenuation dispersion curves versus fluid dynamic viscosity for various frequencies in the case of an elastic surface layer ($\phi \to 0$)

Fig. 11 Phase velocity dispersion curves versus frequency for various fluid dynamic viscosities in the case of a poroelastic surface layer ($\phi = 0.5$)

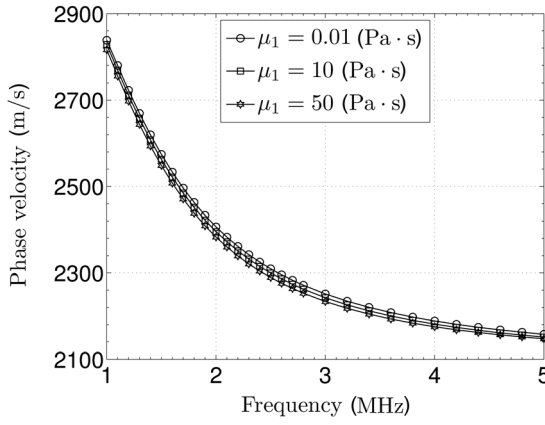**Fig. 9** Phase velocity dispersion curves versus frequency for various fluid dynamic viscosities in the case of an elastic surface layer ($\phi \to 0$)

Fig. 12 Attenuation dispersion curves versus frequency for various fluid dynamic viscosities in the case of an elastic surface layer ($\phi \to 0$)

- Figure 8 shows the attenuation variations versus fluid dynamic viscosity at various frequencies $\left(f = 1, 2, 3, 4, \text{ and } 5 \, (\text{MHz}) \right)$ in the case of an elastic surface layer ($\phi \to 0$). It is seen from this figure that the wave attenuation increases monotonically with increasing dynamic viscosity. Figure 8 shows also that the relationship between attenuation and dynamic viscosity is obviously nonlinear. This figure is identical to that of Ref.
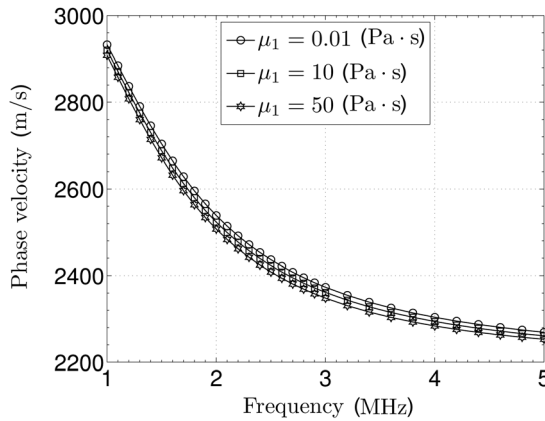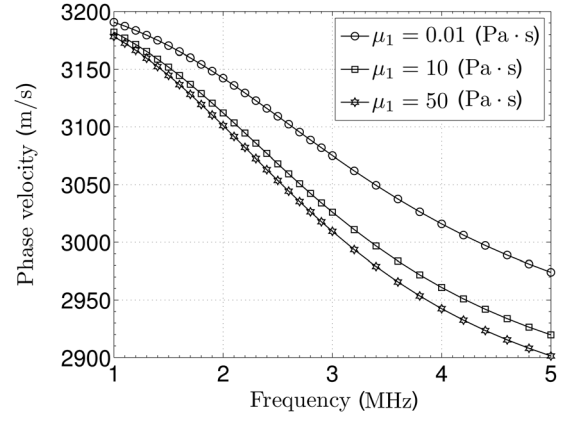
[26]. The new original theoretical resolution is in very good agreement with those of Ref. [26].
- The attenuation dispersion curves in function of frequency were also plotted as shown in Figs. 12–14 for viscosities $\mu_1 = 1, 10, 50, \text{ and } 100 \, (\text{Pa} \cdot \text{s})$. These figures show that the love wave attenuation is a monotonic function of the wave frequency. The Fig. 12 in the case of an elastic surface ($\phi \to 0$) is identical to that of Ref. [26].
- The effect of wave frequency on the attenuation and phase velocity of the love wave is calculated and plotted in Figs. 9–14 for different values of porosity ($\phi \to 0, 0.1, \text{ and } 0.5$). It can be seen from these figures that with increasing wave frequency, the phase velocity decreases and the attenuation increases in a monotonous way. Note that the attenuation and phase velocity for $\phi = 0.5$ are obviously larger than that for ($\phi \to 0$) and $\phi = 0.1$.

3 Conclusions

On the one hand, the propagation of love wave in poroelastic layered with a viscous fluid is investigated using a new original theoretical resolution based on $p - \mathbf{u}$ formulation in this paper. The presence of a viscous fluid on the waveguide surface layer induces losses and causes an attenuation of the surface love wave as it propagates. Furthermore, taking into account of the poroelastic character of the surface makes the mathematical problem much more difficult to solve.

Fig. 10 Phase velocity dispersion curves versus frequency for various fluid dynamic viscosities in the case of a poroelastic surface layer ($\phi = 0.1$)
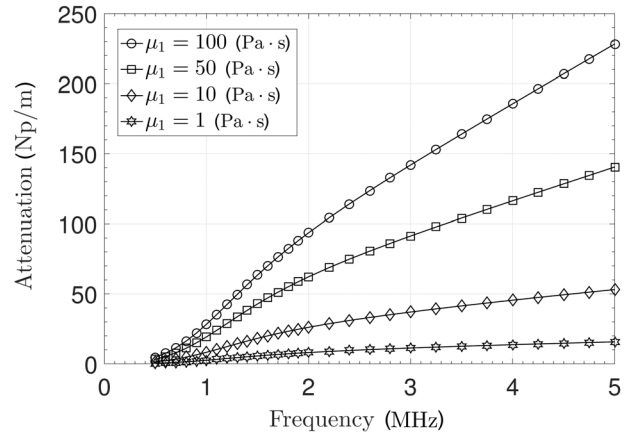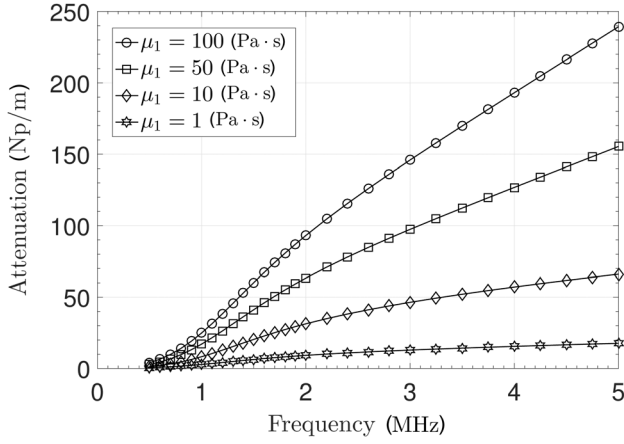
Fig. 13 Attenuation dispersion curves versus frequency for various fluid dynamic viscosities in the case of a poroelastic surface layer ($\phi = 0.1$)
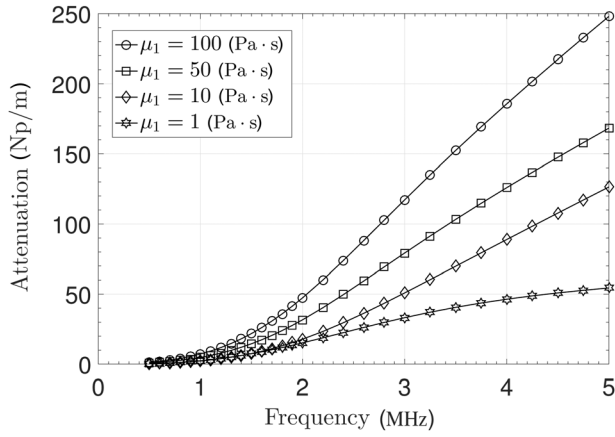

Fig. 14 Attenuation dispersion curves versus frequency for various fluid dynamic viscosities in the case of a poroelastic surface layer ($\phi = 0.5$)

In the other hand, a new theoretical form of the complex dispersion relation of love wave propagation was developed. After a rigorous procedure to separate the complex dispersion relation into real and imaginary parts, the resulting two nonlinear equations were solved. Therefore, the graphs highlighting the behavior of attenuation and phase velocity of love waves versus dynamic viscosity, frequency, and porosity were obtained. It was found that the increase in dynamic viscosity augments the attenuation and reduces the phase velocity of the love wave. It was also found that the increase in porosity augments the attenuation and the phase velocity of the love wave. Finally, the new original theoretical resolution proposed in this work can be used to develop and design the fluid viscosity sensors, in nondestructive testing of materials and in geophysics.

Nomenclature

b = viscous coupling parameter
d = thickness of the poroelastic surface layer
e = dilatation of the solid skeleton
$\mathbf{I}$ = identity tensor
k = permeability of the porous medium
k_r, k_i = real and imaginary parts of the wave number
K_f = pore fluid bulk modulus
K_m = matrix bulk modulus

K_s = solid bulk modulus
m = inertial coupling parameter
M = Biot modulus
p = pore fluid pressure
τ = tortuosity coefficient
ν_1 = kinematic fluid viscosity
$\mathbf{w}$ = relative displacement
α = Biot-Willis coefficient
ζ = volume variations in the fluid
η = pore fluid dynamic viscosity
λ, μ = Lamé constants
μ_2 = shear modulus of the substrate
v_3 = fluid particle velocity in the x_3 direction
ρ_2 = density of the substrate
σ = total stress tensor
ϕ = porosity
ω = angular frequency

Appendix

For typical values of fluid dynamic viscosity (up to 100 (Pa·s)) and frequency (several MHz), the first term in Eq. (17) is much smaller than the corresponding second term. Then, the second terms in Eqs. (15) and (16) are much smaller than the first term. Therefore, the parameters δ, δ_1, and δ_2 given in the Eqs. (17) and (16) can be written in the form

$$\begin{Bmatrix} \delta_1 \\ \delta \\ \delta_2 \end{Bmatrix} = \begin{Bmatrix} A_1 \\ A \\ A_2 \end{Bmatrix} + j \begin{Bmatrix} B_1 \\ B \\ B_2 \end{Bmatrix} \qquad (A1)$$

where

$$A_1 = \frac{1}{\sqrt{2}} \left(\sqrt{\frac{\omega}{\nu_1} - 2k_r k_i} + \frac{k_r^2 - k_i^2}{2\sqrt{\frac{\omega}{\nu_1} - 2k_r k_i}} \right)$$

$$B_1 = \frac{1}{\sqrt{2}} \left(\frac{k_r^2 - k_i^2}{2\sqrt{\frac{\omega}{\nu_1} - 2k_r k_i}} - \sqrt{\frac{\omega}{\nu_1} - 2k_r k_i} \right)$$

$$A = \sqrt{\omega^2 \left[\frac{\rho}{\mu} - \frac{m\rho_f^2}{\mu\left(m^2 + \frac{b^2}{\omega^2}\right)} \right] - k_r^2 + k_i^2}$$

$$B = \frac{\frac{\omega b \rho_f^2}{\mu\left(m^2 + \frac{b^2}{\omega^2}\right)} - 2k_r k_i}{2\sqrt{\omega^2 \left[\frac{\rho}{\mu} - \frac{m\rho_f^2}{\mu\left(m^2 + \frac{b^2}{\omega^2}\right)} \right] - k_r^2 + k_i^2}}$$

$$A_2 = \sqrt{k_r^2 - k_i^2 - \frac{\omega^2}{c_2^2}}$$

$$B_2 = \frac{k_r k_i}{\sqrt{k_r^2 - k_i^2 - \frac{\omega^2}{c_2^2}}}$$

Substituting Eq. (A1) to the complex dispersion relation (20) and grouping the real and imaginary terms, then after elementary manipulations, we obtain

$$F_1 F_3 - F_2 F_4 - F_5 F_7 + F_6 F_8 = 0 \qquad (A2)$$

$$F_2 F_3 + F_1 F_4 + F_5 F_8 + F_6 F_7 = 0 \qquad (A3)$$

where

$$F_1 = \cosh(Bd)\sin(Ad)$$
$$F_2 = \sinh(Bd)\cos(Ad)$$
$$F_3 = \mu^2(A^2 - B^2) - \omega\mu_1\mu_2(A_1 B_2 + B_1 A_2)$$
$$F_4 = 2\mu^2 AB + \omega\mu_1\mu_2(A_1 A_2 - B_1 B_2)$$
$$F_5 = \cos(Ad)\cosh(Bd)$$
$$F_6 = \sin(Ad)\sinh(Bd)$$
$$F_7 = \mu[\omega\mu_1(AB_1 + BA_1) + \mu_2(AA_2 - BB_2)]$$
$$F_8 = \mu[\omega\mu_1(AA_1 - BB_1) - \mu_2(AB_2 + BA_2)]$$

Equations (A2) and (A3) can be written in the form

$$\text{Re}(\text{CDR}) = 0$$
$$\text{Im}(\text{CDR}) = 0 \qquad (A4)$$

This system of two nonlinear Eq. (A4) constitutes the dispersion equations describing surface love wave propagation in the waveguide with a viscous fluid.

References

[1] Kuznetsov, S. V., 2010, "Love Waves in Nondestructive Diagnostics of Layered Composites," Acoust. Phys., **56**(6), pp. 877–892.

[2] Kielczynski, P., and Szalewski, M., 2011, "An Inverse Method for Determining the Elastic Properties of Thin Layers Using Love Surface Waves," Inverse Probl. Sci. Eng., **19**(1), pp. 31–43.

[3] Kielczynski, P., Szalewski, M., Balcerzak, A., and WiejaI, K., 2015, "Group and Phase Velocity of Love Waves Propagating in Elastic Functionally Graded Materials," Arch. Acoust., **40**(2), pp. 273–281.

[4] Safani, J., O'Neill, A., Matsuoka, T., and Yoshinori, S., 2005, "Applications of Love Wave Dispersion for Improved Shear Wave Velocity Imaging," J. Environ. Eng. Geophys., **10**(2), pp. 135–150.

[5] Luo, Y., Xia, J., Liu, J., Liu, Q., and Xu, S., 2007, "Joint Inversion of High Frequency Surface Waves With Fundamental and Higher Modes," J. Appl. Geophys., **62**(4), pp. 375–384.

[6] Luo, Y., Xia, J., Xu, Y., Zeng, C., and Liu, J., 2010, "Finite-Difference Modeling and Dispersion Analysis of High Frequency Love Waves for Near Surface Applications," Pure Appl. Geophys., **167**(12), pp. 1525–1536.

[7] Fukao, Y., and Abe, K., 1971, "Multimode Love Wave Excited by Shallow and Deep Earthquakes," Bull. Earthquake Res. Inst., **49**, pp. 1–12.

[8] Bautista, E. O., and Stoll, R. D., 1995, "Remote Determinations of In Situ Sediment Parameters Using Love Waves," J. Acoust. Soc. Am., **98**(2), pp. 1090–1096.

[9] Boxberger, T., Picozzi, M., and Parolai, S., 2011, "Shallow Geology Characterization Using Rayleigh and Love Wave Dispersion Curves Derived From Seismic Noise Array Measurements," J. Appl. Geophys., **75**(2), pp. 345–354.

[10] Kielczynski, P., and Plowiec, R., 1989, "Determination of the Shear Impedance of Viscoelastic Liquids Using Love and Bleustein-Gulyaev Surface Waves," J. Acoust. Soc. Am., **86**(2), pp. 818–827.

[11] Rostocki, A. J., Siegoczynski, R. M., Kielczynski, P., and Szalewski, M., 2010, "An Application of Love Sh Waves for the Viscosity Measurements of Triglycerides at High Pressures," High Pressure Res., **30**(1), pp. 88–92.

[12] Kielczynski, P., Szalewski, M., Balcerzak, A., Rostocki, A. J., and Tefelski, D., 2011, "Application of Sh Surface Acoustic Waves for Measuring the Viscosity of Liquids in Function of Pressure and Temperature," Ultrasonics, **51**(8), pp. 921–924.

[13] Liu, J., 2014, "A Simple and Accurate Model for Love Wave Based Sensors: Dispersion Equation and Mass Sensitivity," AIP Adv., **4**(7), pp. 1–11.

[14] Raimbault, V., Rebire, D., Dejous, C., Guirardel, M., and Conedera, V., 2008, "Acoustic Love Wave Platform With PDMS Microfluidic Chip," Sens. Actuators A: Phys., **142**(1), pp. 160–165.

[15] Chen, X., and Liu, D., 2010, "Analysis of Viscosity Sensitivity for Liquid Property Detection Applications Based on Saw Sensors," Mater. Sci. Eng.: C, **30**(8), pp. 1175–1182.

[16] Wang, W., Oh, H., Lee, K., and Yang, S., 2008, "Enhanced Sensitivity of Wireless Chemical Sensor Based on Love Wave Mode," Jpn. J. Appl. Phys., **47**(9), pp. 7372–7379.

[17] Hoang, T. B., Hanke, U., Johannessen, E. A., and Johannessen, A., 2016, "Design of a Love Wave Mode Device for Use in a Microfabricated Glucose Sensor," IEEE International Frequency Control Symposium (IFCS), New Orleans, LA, May 9–12, pp. 1–5.

[18] Vikstrm, A., and Voinova, M. V., 2016, "Soft-Film Dynamics of Sh-Saw Sensors in Viscous and Viscoelastic Fluids," Sensing Bio-Sens. Res., **11**(2), pp. 78–85.

[19] Länge, K., Rapp, B. E., and Rapp, M., 2008, "Surface Acoustic Wave Biosensors: A Review," Anal. Bioanal. Chem., **391**(5), pp. 1509–1519.

[20] Oh, H. K., Wang, W., Lee, K., Min, C., and Yang, S., 2009, "The Development of a Wireless Love Wave Biosensor on 41° YX LiNbO$_3$," Smart Mater. Struct., **18**(2), p. 025008.

[21] Pramanik, A., and Gupta, S., 2016, "Propagation of Love Waves in Composite Layered Structures Loaded With Viscous Liquid," Procedia Eng., **144**, pp. 461–467.

[22] Du, J., Xian, J., Wang, J., and Yong, Y. K., 2008, "Propagation of Love Waves in Prestressed Piezoelectric Layered Structures Loaded With Viscous Liquid," Acta Mech. Solida Sin., **21**(6), pp. 542–548.

[23] Kim, J. O., 1992, "The Effect of a Viscous Fluid on Love Waves in a Layered Media," J. Acoust. Soc. Am., **91**(6), pp. 3099–3103.

[24] Wu, T. T., and Wu, T. Y., 2000, "Surface Waves in Coated Anisotropic Medium Loaded With Viscous Liquid," ASME J. Appl. Mech., **67**(2), pp. 262–266.

[25] Guo, F. L., and Sun, R., 2008, "Propagation of Bleustein-Gulyaev Wave in 6 mm Piezoelectric Materials Loaded With Viscous Liquid," Int. J. Solids Struct., **45**(13), pp. 3699–3710.

[26] Kielczynski, P., Szalewski, M., and Balcerzak, A., 2012, "Effect of a Viscous Liquid Loading on Love Wave Propagation," Int. J. Solids Struct., **49**(17), pp. 2314–2319.

[27] McMullan, C., Mehta, H., Gizeli, E., and Lowe, C. R., 2000, "Modeling of the Mass Sensitivity of the Love Wave Device in the Presence of a Viscous Liquid," J. Phys. D: Appl. Phys., **33**(23), pp. 3053–3059.

[28] Biot, M. A., 1956, "Theory of Propagation of Elastic Waves in a Fluid-Saturated Porous Solid—I: Low-Frequency Range," J. Acoust. Soc. Am., **28**(2), pp. 168–178.

[29] Biot, M. A., 1956, "Theory of Propagation of Elastic Waves in a Fluid Saturated Porous Solid—II: Higher Frequency Range," J. Acoust. Soc. Am., **28**(2), pp. 179–191.

[30] Biot, M. A., 1962, "Mechanics of Deformation and Acoustic Propagation in Porous Media," J. Appl. Phys., **33**(4), pp. 1482–1498.

[31] Biot, M. A., 1962, "Generalized Theory of Acoustic Propagation in Porous Dissipative Media," J. Acoust. Soc. Am., **34**(9A), pp. 1254–1264.

[32] Wang, H. F., 2000, *Theory of Linear Poroelasticity With Applications to Geomechanics and Hydrogeology*, Princeton University Press, Princeton, NJ.

[33] Biot, M. A., and Willis, D. G., 1957, "The Elastic Coefficients of the Theory of Consolidation," ASME J. Appl. Mech., **24**, pp. 594–601.

[34] Hickey, C. J., and Sabatier, J. M., 1997, "Choosing Biot Parameters for Modeling Water-Saturated Sand," J. Acoust. Soc. Am., **102**(3), pp. 1480–1484.

[35] Stoll, R. D., 1974, "Acoustic Waves in Saturated Sediments," *Physics of Sound in Marine Sediments. Marine Science*, L. Hampton, ed., Springer, Boston, MA.

[36] Morse, P. M., and Feshbach, H., 1946, *Methods of Theoretical Physics Part II*, McGraw-Hill, New York.

[37] Achenbach, J. D., 1973, *Wave Propagation in Elastic Solids*, North-Holland Publishing, Amsterdam, The Netherlands.

[38] Zheng, P., Zhao, S. X., and Ding, D., 2013, "Dynamic Green's Function for a Poroelastic Half-Space," Acta Mech., **224**(1), pp. 17–39.